Small Anion with Higher Valency Retards the Compaction of DNA in the Presence of Multivalent Cation

Takuya Saito,[†] Takafumi Iwaki,[‡] and Kenichi Yoshikawa[†§*]

[†]Department of Physics, Graduate School of Science, Kyoto University, Kyoto, Japan; [‡]Okayama Institute for Quantum Physics, Okayama, Japan; and [§]Spatio-Temporal Order Project, International Cooperative Research Project, Japan Science and Technology Agency, Kyoto University, Kyoto, Japan

ABSTRACT It has been established that, upon the addition of multivalent cations, long DNA chains in an aqueous solution exhibit a remarkable discrete transition from a coil state to a compact state at the level of a single chain. In this study, we investigated the polyelectrolyte nature of DNA with the experimental methodology of single-DNA observation, and provide a theoretical interpretation. We examined the effects of co-ions with different valencies (Cl^-, SO_4^{2-}, PO_4^{3-}) on DNA compaction. As a result, we found that co-ions with a greater valency induce the coil state rather than the compact state. Based on a simple model with mean-field approximation that considered ion pairing, we show how the increase in entropy of small ions contributes to the stability of the compact state, by overcoming entropic penalties such as elastic confinement of the chain and a decrease in the translational freedom of counterions accompanied by charge neutralization.

INTRODUCTION

In a many-body Coulomb system, the coexistence of asymmetric charges with different sizes and valencies is a fascinating subject. A typical example is a living cellular system, in which negatively charged DNA molecules are confined into a small space that contains various small ions to counter the negative charge of DNA. Therefore, it is necessary to gain insight into the structure of DNA in terms of a multiple-component asymmetric Coulomb system. In addition, our understanding of the folding transition of a polyelectrolyte is still primitive, compared to what we know of the manner of dispersion/aggregation of charged colloids (1,2).

Through in vitro experiments, it has been shown that the addition of multivalent cations induces a remarkable compacting transition of DNA accompanied by a change in volume on the order of 10^4 (3,4). The minimum system for observing such a transition consists of DNA, water, multivalent counterions, and co-ions. Usually, monovalent counterions, such as potassium and sodium ions, are also added to mimic the environment of an intracellular solution.

Moreover, based on monomolecular observations of DNA by fluorescent microscopy, it has been confirmed that a single DNA chain undergoes a large discrete compacting transition (5). This transition is characterized as a first-order phase transition under the criterion of Landau's symmetry argument, which reflects the semiflexible nature of a giant DNA molecule. Such a characterization is also supported by experimental observations that compact DNA takes an ordered state, while coiled DNA takes a disordered state (6,7). The elastic entropy of the chain in the disordered coil state is clearly greater than that in the ordered compact state. At first glance, this seems to give a situation in which a compact phase appears at low temperature in a phase diagram. However, in DNA compaction induced by multivalent cations, the compact state is more stable than the coil state when the temperature is increased (8–10), which means that the ordered compact state shows greater entropy than the elongated coil state. This discrepancy indicates that some other essential factors influence this phenomenon.

The free energy in a DNA molecule bathing in a solution can be written as

$$F = F_{\mathrm{ela}} + F_{\mathrm{tra}} + F_{\mathrm{ele-st}}, \qquad (1)$$

where the first term is the elastic free energy of the DNA chain, the second term is the contribution of the translational entropy of small ions, and the last term is the electrostatic free energy. Entropy is predominantly influenced by the elastic and translational terms. The above-mentioned temperature-dependence would be attributable to the translational entropy, since the elastic entropy decreases during the ordered packing of a DNA chain. On the other hand, the origin of the loss in enthalpy is not as clear. The change in translational entropy upon compaction is associated with the formation or deformation of ion clusters, which is the bound state of ionic species. For this multiple-component system, we can consider ion coupling between DNA and counterions, and between counterions and co-ions (especially multivalent cations and anions). If this system only contained ion clusters between DNA and counterions, it would be a delicate problem to explain the temperature-dependence of DNA compaction, since the coupling with counterions that is promoted along with compaction should give a gain in enthalpy. However, the ion cluster between counterions and co-ions could explain the experimental results with regard to both entropy and enthalpy, since the

Submitted August 25, 2008, and accepted for publication November 5, 2008.

*Correspondence: yoshikaw@scphys.kyoto-u.ac.jp

Takuya Saito's present address is Department of Mechanical Engineering, School of Engineering, The University of Tokyo.

Editor: David P. Millar.

0006-3495/09/02/1068/8 $2.00

doi: 10.1016/j.bpj.2008.11.008

exchange from ion pairs to multivalent cations upon compaction, i.e., the release of co-ions, could cause a loss of electrostatic energy and a gain in translational entropy. Furthermore, the balance of the concentrations of ion pairs and multivalent cations in the bulk could make a crucial contribution to this ionic exchange around DNA. If such electrostatic correlation between different charged species does have a significant contribution, then we could expect that the transition of DNA would greatly change with a change in the valency of co-ions.

In this study, to investigate the effect of such correlation among different ions, we examined the effect of the valency of co-ions in DNA compaction induced by multivalent cations (spermine(4^+)). For this purpose, we performed monomolecular observations in the presence of NaCl, Na_2SO_4, or Na_3PO_4. We propose a simple theoretical model of DNA compaction that accounts for the experimental trends with regard to both co-ion valency and temperature.

EXPERIMENTS

Single DNA molecules were observed by fluorescence microscopy. We used an Axiovert 135 (Carl Zeiss, Jena, Germany) equipped with EB-CCD cameras (Hamamatsu Photonics, Hamamatsu City, Japan). Samples were prepared as follows: Bacteriophage T4DNA (166 kbp, Nippon Gene, Toyama, Japan) was dissolved at 0.1 μM (in base units) in 0.1 μM of the fluorescent dye 4′6-diamidino-2-phenylindole (Wako Pure Chemical Industries, Osaka, Japan). Spermine in chloride form (Nakalai Tesque, Kyoto, Japan) was added as a multivalent cation. For this experiment, NaCl, Na_2SO_4, and Na_3PO_4 (analytical grade) were used.

RESULTS

Fig. 1 shows examples of the conformations of DNA chains with 10 mM NaCl under different concentrations of spermine(4^+) as observed by fluorescence microscopy. From top to bottom, the figures correspond to fluorescence images of DNA (Fig. 1 *a*), their schematic representations (Fig. 1 *b*), a quasi-three-dimensional representation of the fluorescence intensity (Fig. 1 *c*), and histograms of the long-axis lengths of DNA in each solution (Fig. 1 *d*), respectively. The left and right columns show the regions where all of the DNA chains are in the coiled and compact states, respectively. The middle column shows the coexistence of the coiled and compact states. These results indicate that DNA compaction is a discrete transition at the level of a single chain (5). In fact, it has been confirmed that this compaction phenomenon can be characterized as a first-order phase transition under the criterion of Landau's symmetry argument.

Next, we examined the concentration effects of monovalent cations (Na^+). Fig. 2 shows phase diagrams of the DNA conformation on the [Na^+]-[spermine(4^+)] plane in the presence of monovalent (Fig. 2 *a*), divalent (Fig. 2 *b*), and trivalent anions (Fig. 2 *c*) (Cl^-, SO_4^{2-}, and PO_4^{3-}, respectively). Under these experimental conditions, anion concentrations are 1), equal; 2), one-half; and 3), one-third with respect to [Na^+], respectively. Circles show the experimental results and lines correspond to the theoretical estimations of the phase boundary, which is discussed later. From these results, it is evident that, with an increase in the concentration of monovalent cation, the concentration of spermine(4^+) needed to induce compaction increases. This means that the addition of monovalent cation inhibits DNA compaction by spermine(4^+).

On the other hand, the phase boundary shifts toward the region of a compact state when the anionic valency increases. This indicates that the DNA compaction induced by multivalent cation is retarded in the presence of anions with higher valencies.

DISCUSSION

To discuss the thermodynamics of DNA compaction, it is necessary to know the ion distribution in solution in detail. While the equilibrium ion distribution has been traditionally discussed by the Debye-Hückel theory (11), this theory does not give the correct ion distribution around a highly charged polymer, where the assumption of a weak electric field is not valid. This problem has been studied by the nonlinear Poisson-Boltzmann equation (12) or the mean field theory based on a two-state approximation (counterion condensation theory) (13,14). Unfortunately, these theories do not completely describe an ion solution. For example, they do not include the attractive effective force between polyelectrolytes. They also do not explain the temperature-dependence of DNA compaction, even in a qualitative manner. These have been difficult and delicate problems associated with polyelectrolyte condensation. In this study, we tried to explain especially the latter problem together with the dependence on the co-ion valency by modifying the theory of compaction based on the counterion condensation theory.

The electrostatic correlation on a macroscopic scale as in the framework of the Debye-Hückel theory provides adequate phenomenology in many cases. A defect in conventional theories would partially arise from a one-particle approximation that ignores the ion correlation on a microscopic scale, i.e., the contribution from an ion cluster. This contribution seems to be particularly important when high-valency ions play an essential role in the condensation phenomenon. In fact, the effect of co-ions in the folding transition of DNA induced by PEG and monovalent counterions can be well explained in terms of the electrostatic free energy between counterions and Debye's screening atmosphere (15). However, this contribution is too small to explain the order of the shift of transition points observed in this experiment on compaction induced by multivalent counterions.

Here, we propose a model that directly considers the ion pair between a counterion and a co-ion as one of the

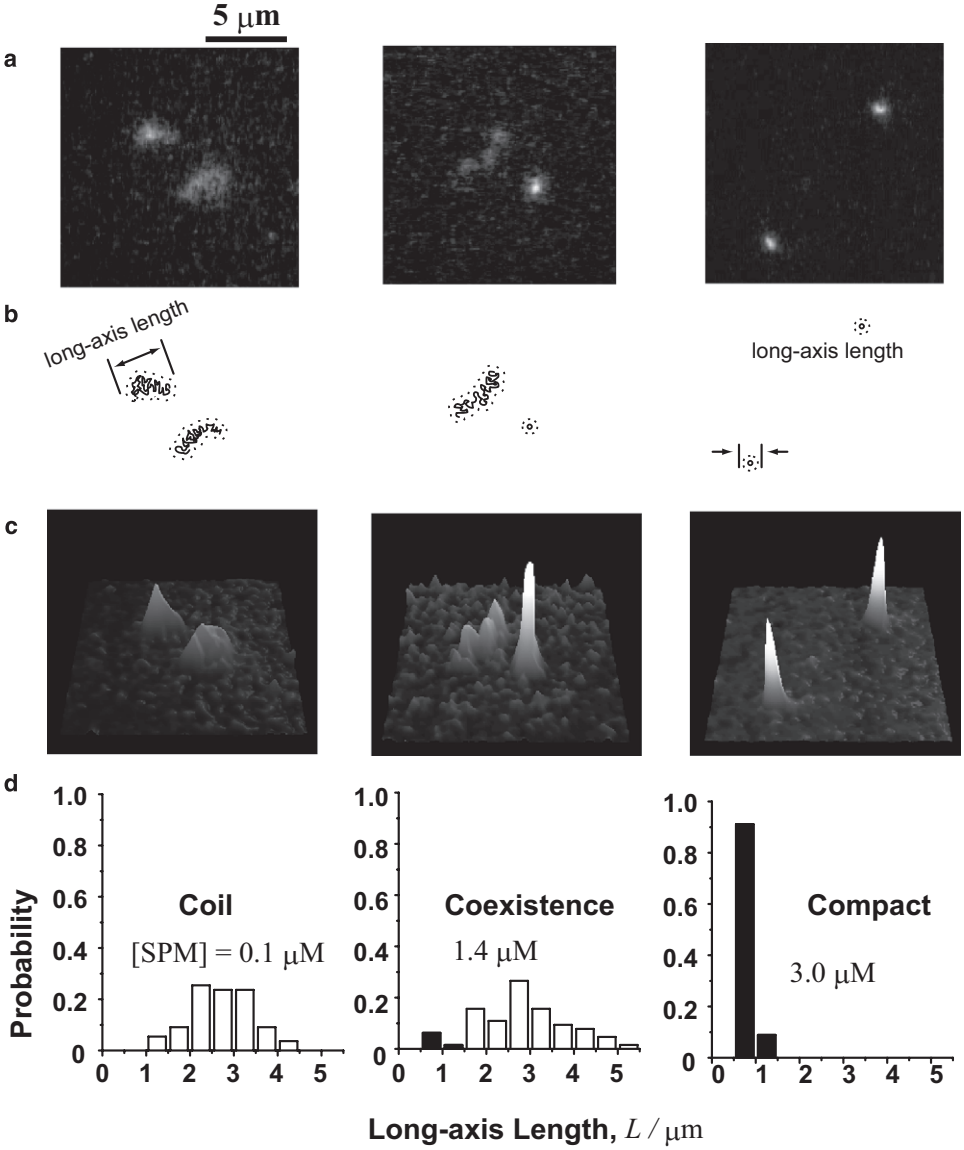

FIGURE 1 (*a*) Fluorescence microscopic images of T4 DNA. The salt conditions for the left, middle, and right are 0.1 μM, 1.5 μM, and 3.0 μM spermine, respectively, at a fixed 10 mM NaCl. (*b*) Schematic images of the actual conformation of DNA with a blurring effect represented by dashed surroundings. (*c*) Quasi-three-dimensional representations correspond to the fluorescence images, respectively. The height in the quasi-three-dimensional representations corresponds to the intensity in the fluorescence images. (*d*) Histogram of long-axis length in 0.1 μM, 1.4 μM, and 3.0 μM spermine from left to right, respectively, at a fixed 10 mM NaCl. The solid and open bars indicate the compact and coil states, respectively.

components in the system, as shown in Fig. 3. In this setting, the monovalent cations, multivalent cations, and ion pairs are condensed in the vicinity of the coiled DNA. On the other hand, compact DNA is almost neutralized by multivalent cations.

The free energy of a single DNA chain can be written as

$$F = F_{\mathrm{ela}} + F_{\mathrm{el,c}} + F_{\mathrm{bind}} + F_{\mathrm{t-p}}, \qquad (2)$$

where F_{ela} is the elastic free energy of a DNA chain, $F_{\mathrm{el,c}}$ is the electrostatic free energy in the surface ion atmosphere around the counterion condensation region on DNA, F_{bind} represents an electrostatic binding free energy between DNA segments mediated by multivalent cations, and $F_{\mathrm{t-p}}$ is the contribution from the difference in the free energy of small ions and ion pairs between the condensed region and bulk (translational entropy and electrostatic energy of ion pairs). In this study, we consider DNA as a polyelectrolyte with a length Qd, carrying a charge Qe, where e is the unit charge, Q is the total number of unit charges on DNA, and d is the interval distance between unit charges on DNA. This chain has a thickness with a radius a_{DNA}, around which small ions condense with thickness Δa. This means that the condensed volume of small ions around DNA per unit charge is $v \equiv \pi(a_{\mathrm{D}} + \Delta a)^2 d - \pi {a_{\mathrm{D}}}^2 d$. The fraction of condensed small ions per unit charge is $\{\theta_{\mathrm{i}}\}$. Index $\{i\}$ represents M^{+}, 1^{+}, a^{-}, and p, which denote the multivalent cations, monovalent cations, co-ions, and the ion pair, respectively. The DNA molecule is also dissolved in the salt solution, where $\{c_{\mathrm{i}}\}$ is the net bulk concentration of small ions with valency $\{z_{\mathrm{i}}\}$.

Bulk solution

First, we determine the equilibrium of small ions in bulk. We consider a system with volume, V, containing $\{N_{\mathrm{i}}\}$, ionic

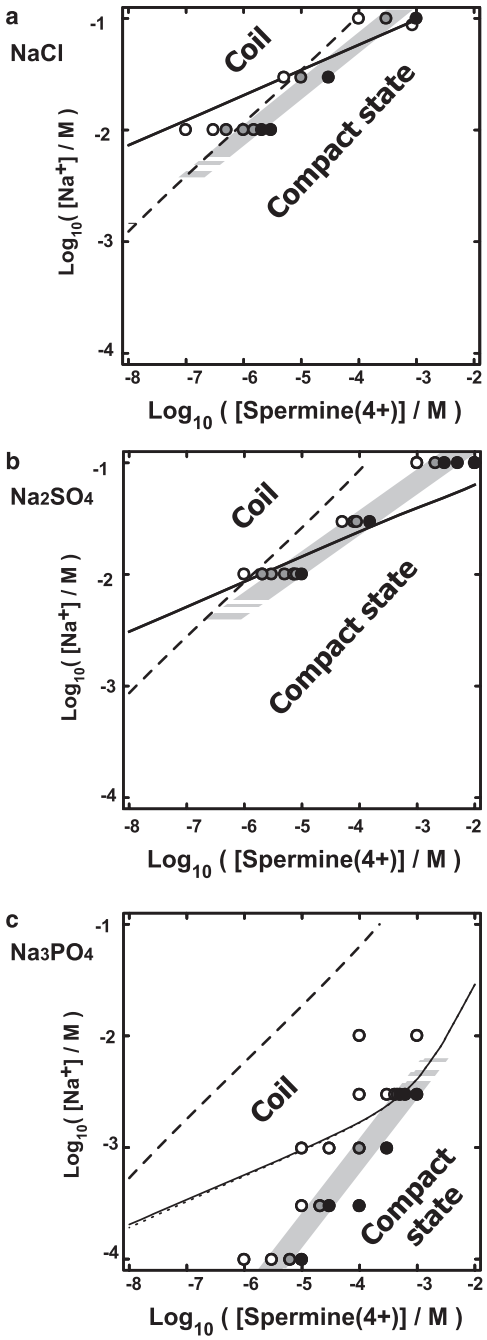

FIGURE 2 Phase diagram in DNA compaction on the $[Na^+]$-[spermine(4^+)] plane, obtained from experimental and theoretical results in the presence of (*a*) Cl^-, (*b*) SO_4^{2-}, and (*c*) PO_4^{3-}, respectively. The open, solid, and shaded circles indicate the experimental results in the regions of the coil state, compact state, and their coexistence, respectively. The shaded regions, which represent coexistence, are visual guides for the experimental results. The solid and dashed lines indicate the theoretical phase boundary in the model with ion pairing at $\beta(\Delta f_{ela} + \Delta f_{bind}) = -2.0$ and that without ion pairing at $\beta(\Delta f_{ela} + \Delta f_{bind}) = -1.1$, respectively. The dotted line in panel *c* shows the theoretical phase boundary in which the effect of the change in the persistence length is taken into account. These calculations were performed with the following parameters: $d = 0.17$ nm, $l_B = 0.71$ nm, $l_{p,0} = 50$ nm, $a_D = 1$ nm, $\Delta a = 0.5$ nm, $a_p = |z_{M^+} z_{a^-} l_B|$, $\bar{a} = 0.18$, 0.31, and 0.27 nm at $z_a^- = -1$, -2, and -3, respectively.

species, respectively. These small ions satisfy the conservation of the particle number, $N_{M^+} + N_p = N^*_{M^+}$, $N_{a^-} + N_p = N^*_{a^-}$, where $N^*_{M^+}$, $N^*_{a^-}$ represent the number of total ions in the system. Let F_{t-p} be the free energy of the bulk. This free energy can be described as the sum of the translational entropy of small ions and the internal free energy of ion pairs,

$$\begin{aligned}\beta F_{t-p} &= (N^*_{M^+} - N_p)\log[(N^*_{M^+} - N_p)/eV] \\ &+ (N^*_{a^-} - N_p)\log[(N^*_{a^-} - N_p)/eV] \\ &+ N_p \log[N_p/eV] - N_p \log\zeta \\ &+ N_{1^+}\log[N_{1^+}/eV],\end{aligned} \tag{3}$$

where $\beta = 1/k_B T$ (k_B is the Boltzmann constant, T is the absolute temperature), and the internal partition function of ion pairing is

$$\zeta \equiv \int_{\bar{a}}^{a_p} dr 4\pi r^2 \exp[-\psi(r)], \tag{4}$$

where $\psi(r) = l_B z_{M^+} z_{a^-}(1/r - 1/a_p)$, $\bar{a}$ is the distance of closest approach between monovalent cation and anion, a_p is the cutoff distance of the ion pair, and $l_B \equiv e^2/\varepsilon k_B T$ is the Bjerrum length (ε is the dielectric constant). The paired state of ions is introduced by analogy with Bjerrum pair (16), although the ion pairs are not neutralized in this system. For simplicity, we neglect the gain in the electrostatic free energy of the Debye-Hückel screening atmosphere in bulk, since the dimension of ion pairs should be much smaller than the Debye-Hückel screening length at this lower

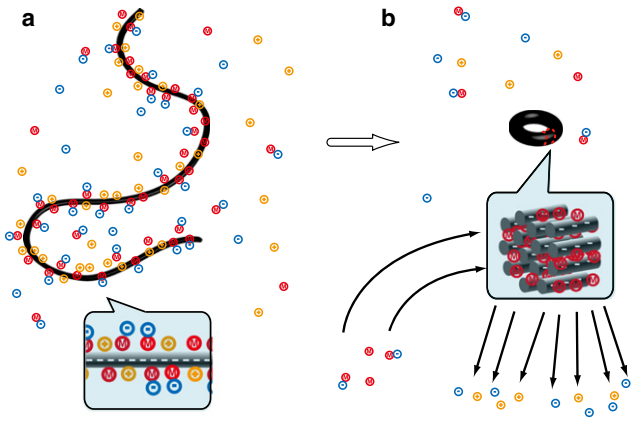

FIGURE 3 (Color online) Schematic representation of the ion distribution with ion pairs in the (*a*) coil and (*b*) compact states, respectively. The red spheres represented by M, orange spheres represented by +, and blue spheres represented by −, indicate multivalent cation, monovalent cation, and co-ion, respectively. (*a*) In the coil state, the small ions are condensed in the close vicinity of DNA. Moreover, some co-ions are condensed as ion pairs with multivalent cations. (*b*) In the compact state, compacted DNA is neutralized by multivalent cations. In these images, co-ions and monovalent cations are released into the bulk with compaction. In addition, in the model without ion pairs, the ion distribution is represented as the substitution from ion pairs (M, −) to bare multivalent cations (M).

concentration of salt. In fact, upon DNA compaction, Debye-Hückel screening is too small to explain the transition shift as shown in the calculation (15), compared with the following result.

We minimize Eq. 3 with respect to N_p. Thus, we have the mass action law as

$$N_{M^+}N_{a^-} = N_pV/\zeta,\ \left(c_{M^+}c_{a^-} = c_p/\zeta\right), \tag{5}$$

where $c_i \equiv N_i/V$. The bulk concentration of the ion pair is explicitly written as

$$c_p = \alpha - \sqrt{\alpha^2 - c^*_{M^+}c^*_{a^-}}, \tag{6}$$

where $\alpha = (c^*_{M^+} + c^*_{a^-} + 1/\zeta)/2$. Note that we take a minus sign before a square root, since $c_p = c^*_{M^+}$ if $1/\zeta = 0$.

Equation 3 is also written as

$$\beta F_{t-p} \equiv \sum_{k=\left\{M^+,p,1^+,a^-\right\}} N_k \log(N_k/eV) - N_p \log\zeta. \tag{7}$$

Here, we introduce the chemical potential of small ions and ion pairs in bulk as $\mu_k \equiv \partial F_{t-p}/\partial N_k$. This leads to $\mu_k = k_BT\log(c_k)$ ($k = \{M^+, 1^+, a^-\}$) and $\mu_p = k_BT\log(c_p) - k_BT\log\zeta$. Note that the chemical potential does not depend on the condensed number of small ions in DNA, since the number of small ions in bulk is very large compared with the charge of DNA, and this acts as a particle bath for DNA. In addition, to make clear the role of ion parings between multivalent cations and co-ions, we do not consider pK_b and pK_a as well as pH, although they should be nonnegligible factors, especially for the case of phosphate ions.

Coiled DNA

By using the above net concentration, we consider the free energy of a monomolecular DNA chain in a coil state. In this case, the contributions to the free energy can be given as follows:

$$\beta F^{coil}_{ela} = const., \tag{8}$$

$$\beta F^{coil}_{el,c} = Q\left(1 - \sum_{j=\{M^+,1^+,p\}} z_j\theta^{coil}_j\right)^2 \times \frac{l_B}{\kappa(a_D + \Delta a)d}\frac{K_0[\kappa(a_D + \Delta a)]}{K_1[\kappa(a_D + \Delta a)]}, \tag{9}$$

$$\beta F^{coil}_{t-p} = Q\sum_{j=\left\{M^+,p,1^+\right\}} \theta^{coil}_j \log\left(\theta^{coil}_j/ec_jv\right), \tag{10}$$

where the Debye length is $\kappa^{-1} \equiv (4\pi l_B\sum_i z_i^2c_i)^{-\frac{1}{2}}$, and *const.* in this article means $\partial F_{xxx}/\partial c_i \equiv 0$ and $\partial F_{xxx}/\partial z_{a^-} = 0$. The independence of F^{coil}_{ela} on c_i for all i and z_{a^-} is justified when the Debye length is small enough to make the electrostatic persistence length much smaller than the intrinsic one (17,18). The screening electrostatic free energy in Eq. 9 is derived as described in the literature (19). For the coil state, the term F^{coil}_{bind} does not exist. F_{t-p} is originally defined as follows:

$$\beta F_{t-p} \equiv -\beta\sum_{k=\left\{M^+,p,1^+\right\}} Q\theta_k\mu_k + \sum_{k=\left\{M^+,p,1^+\right\}} Q\theta_k\log[\theta_k/ev] - Q\theta_p\log\zeta. \tag{11}$$

Although Eq. 11 finally takes the form of the translational entropy, apparently as in Eq. 10, this term includes enthalpy, since c_{M^+}, c_{a^-}, and c_p depend on temperature. Based on the concept of a two-state model (13,14), the fraction of condensed counterion, $\{\theta^{coil}_j\}$, is determined by minimization of the Eqs. 9 and 10.

Compact DNA

Next, we consider the compact state of DNA,

$$\beta F^{comp}_{ela} = const., \tag{12}$$

$$\beta F^{comp}_{el,c} = 0, \tag{13}$$

$$\beta F^{comp}_{bind} = const.\ (<0), \tag{14}$$

$$\beta F^{comp}_{t-p} = Q(1/z_{M^+})\log(1/z_{M^+}ec_{M^+}v), \tag{15}$$

where the index ''comp'' indicates the compact state. It is difficult to determine the exact details of this state. We can discuss a rough estimation of the free energy by assuming that compact DNA is almost completely electrically neutralized by multivalent cations. This means that $\theta_{M^+} = 1/z_{M^+}$, $\theta_{1^+} = 0$, and $\theta_p = 0$. In principle, the residual charge of a DNA-cation complex leads to electrostatic energy to make the compact state unstable. Thus, it is expected that the interior of a DNA condensate is significantly electrically neutralized. In fact, the experimental result in the presence of multivalent cation supports this expectation (20). Furthermore, multivalent ions interact more strongly than monovalent ions (13,21–28). When nonlinearity is nonnegligible, as in counterion condensation, this tendency should be further intensified. The change in free energy that accompanies compaction can be discussed in terms of two ideal steps. In the first step, ion-exchange occurs and DNA is fully neutralized by only multivalent cations. In the second step, an attractive effective interaction arising from some correlation effect adheres DNA segments to each other. F_{bind} represents a gain in the free energy arising in this latter step. The details of this term are not discussed in this article. In Eq. 12, the independence of the elastic free energy in compact DNA on the salt concentration and co-ion valency is justified under the same conditions as discussed in the case of coiled DNA. Note that the elastic free energy in compact DNA is larger than that in coiled DNA.

Transition points on the [Na^+]-[spermine(4^+)] plane

Here, we estimate the critical concentrations for different co-ion valencies. The free energy of the coil state is equal to that of the compact state at the critical concentration (transition point),

$$\sum_{xxx} F_{xxx}^{coil} = \sum_{xxx} F_{xxx}^{comp}, \tag{16}$$

where "xxx" represents indexes in all contributions. Equation 16 can be transformed as

$$\Delta F_{el,c} + \Delta F_{t-p} = -\Delta F_{ela} - \Delta F_{bind}. \tag{17}$$

The control parameters in this experiment are the co-ion valency and the concentrations of small ions. In Eq. 17, the left-hand side depends on these parameters, while the right-hand side does not. Therefore, if we substitute a certain adequate constant for the right-hand side, Eq. 17 gives the phase boundary as a function of the concentrations of multivalent and monovalent cations.

The experiment shows that compaction is inhibited by the addition of monovalent salt, and this inhibiting effect is enhanced by an increase in the valency of co-ions. Fig. 2 shows a theoretical phase boundary determined by Eq. 17, for comparison with the experimental results. The constant for the right-hand side in Eq. 17 is $\Delta f_{el,c} + \Delta f_{t-p} = +2.0$ with ion pairing, $\Delta f_{el,c} + \Delta f_{t-p} = +1.1$ without ion pairing, where we define $f_{xxx} \equiv F_{xxx}/Q$ as the free energy divided by the total charge of DNA. In the model considering no ion pairing, $\{\theta_j^{coil}\}$ is determined from minimization if we ignore the terms c_p and θ_p. In this case, the theoretical phase boundary is insensitive to the co-ion valences, unlike the model considering ion pairing. The correspondence between the theoretical lines and experimental results in the model considering ion pairing suggests that ion pairing between a co-ion and a multivalent counterion is essential for the understanding of the effect of co-ion valency.

The experimental trend is explained as follows: When the concentration of salt increases, the concentration of monovalent cations in the bulk increases. In this case, the release of monovalent cations from DNA to the bulk is inhibited. This release is considered to be one of the main processes in DNA compaction induced by multivalent cations, and thus compaction itself is inhibited. When the concentration of multivalent cations increases, the adsorption of multivalent cations onto DNA is promoted. This is the counterpart of the ion exchange between multivalent and monovalent cations that accompanies the DNA compaction process. Consequently, compaction is promoted by the addition of multivalent cations.

How does the presence of ion pairs influence the above scenario? Based on this model, several ion pairs are condensed on coiled DNA. In the process of DNA compaction, these ion pairs are released along with monovalent counterions. When the concentration of salt increases, the equilibrium shifts to increase the number of ion pairs, which inhibits compaction. Moreover, the increase in ion pairs means a decrease in multivalent counterions in the bulk, which also inhibits DNA compaction. In principle, the presence of ion pairs enhances the inhibiting effect of the salt on DNA compaction. When the concentration of multivalent cations increases, the equilibrium shifts to increase the number of ion pairs. As discussed above, the increase in ion pairs inhibits compaction, and this makes compaction relatively insensitive to the addition of multivalent cations.

Furthermore, the above scenario is applicable to the valency effect of co-ions. Basically, the concentration of multivalent cations decreases with an increase in co-ion valency due to the stronger electrostatic interaction. Therefore, a co-ion with a higher valency has an inhibitory effect.

Changes in entropy and enthalpy that accompany DNA compaction

Finally, we show that this model involving the formation of ion pairs is consistent with the typical temperature-dependence of DNA compaction. In condensation induced by multivalent cations, compact DNA is favored when the temperature increases (8–10). This indicates that there is a gain in entropy and a loss in enthalpy upon compaction.

Fig. 4 shows the theoretical profiles of the change in entropy in $S_{el,c} + S_{t-p}$ upon the transition, considering ((Fig. 4 *a*) the formation of ion pairs and (Fig. 4 *b*) no formation of ion pairs, respectively, in the presence of monovalent anion (1:1 salt). These profiles are calculated with the same parameters as in Fig. 2 from

$$\Delta\left(S_{el,c} + S_{t-p}\right) \equiv -\partial\left(\Delta F_{el,c} + \Delta F_{t-p}\right)/\partial T, \tag{18}$$

where entropy is defined as $S_{xxx} \equiv -\partial(F_{xxx})/\partial T$, ($\Delta s_{xxx} \equiv \Delta S_{xxx}/Q$). In the case of no ion pairs, the ion distribution in coiled DNA $\{\theta_j^{coil}\}$ is obtained by the same procedure as in Transition Points on the [Na^+]-[Spermine(4^+)] Plane.

As shown in Fig. 4 *a*, the change in entropy around the transition line has a positive value when we consider the formation of ion pairs. However, when there are no ion pairs, this change in entropy is negative everywhere in Fig. 4 *b*.

To discuss the consistency of the total change in enthalpy and entropy in the model with ion pairs, we estimate the change in entropy and enthalpy when $\Delta F_{ela} + \Delta F_{bind} = -2.0\ Qk_BT$ ($\simeq -7 \times 10^5\ k_BT$) as in Fig. 2. For the elastic free energy, the entropic contribution should be dominant, since it can be obtained from the Flory formula, $\beta F_{ela} = \frac{3}{2}\left((R/N^{1/2}a)^2 + (R/N^{1/2}a)^{-2}\right)$, where R is the effective spatial radius such as the hydrodynamic radius, N is the segment number of DNA, and a is the Kuhn length. By using the experimental value of the hydrodynamic radius (29), we approximately obtain $\Delta S_{ela} \approx -10^3 k_B$. Thus, we have $\Delta F_{bind} \approx -2.0\ Qk_BT + 1000\ k_BT \approx -7 \times 10^5\ k_BT$. On the other hand, we estimate the change in entropy on the left-hand side in Eq. 17 from Fig. 4. On the transition line, we

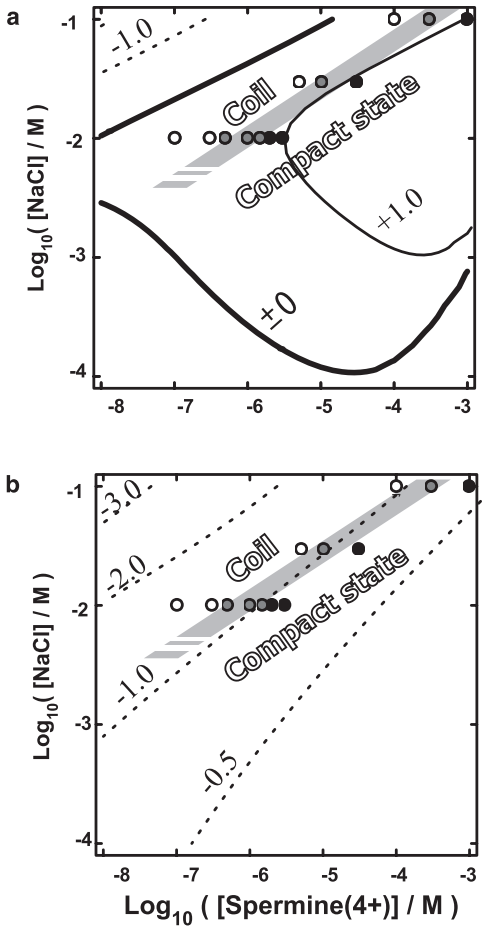

FIGURE 4 Diagram of the theoretical change in entropy, and the change in the conformation of DNA obtained from experimental results in the presence of monovalent anion, on the [NaCl]-[spermine(4^+)] plane. (*a* and *b*) Models with and without ion pairs, respectively, while the experimental results in panels *a* and *b* are the same. The solid and dotted lines show the nonnegative and negative apparent changes in entropy of small ions upon compaction per unit charge of DNA, $(\Delta s_{\mathrm{el,c}} + \Delta s_{\mathrm{tra}})/k_{\mathrm{B}}$. The parameters in the calculations and the experimental results are the same as those in Fig. 2.

approximately obtain $\Delta S_{\mathrm{el,\,c}} + \Delta S_{\mathrm{t-p}} \approx +0.5\,Qk_{\mathrm{B}} \approx +10^5\,k_{\mathrm{B}}$, and $\Delta H_{\mathrm{el,\,c}} + \Delta H_{\mathrm{t-p}} \approx +2.5\,Qk_{\mathrm{B}}T \approx +8 \times 10^5\,k_{\mathrm{B}}T$. In this case, if the contribution in ΔF_{bind} is almost completely occupied by an enthalpy component, the loss in enthalpy $\Delta H_{\mathrm{el,\,c}} + \Delta H_{\mathrm{t-p}}$ overcomes the gain in enthalpy of binding ΔH_{bind}. This means that the total change in enthalpy reflects the loss upon compaction. Furthermore, the entropic contribution of small ions, $\Delta S_{\mathrm{el,\,c}} + \Delta S_{\mathrm{t-p}}$, overcomes the loss in elastic entropy. Thus, this result corresponds to the changes in both enthalpy and entropy in the experimental results regarding temperature-dependence.

The reason for the positive gain in entropy shown above can be associated with the gain in entropy and loss in enthalpy accompanied by the dissociation of ion pairs released in the bulk. However, the temperature-dependence itself can be explained from a simpler perspective, as follows: The temperature derivative of c_{p} is given by

$$\frac{\partial c_{\mathrm{p}}}{\partial T} = \frac{\partial \zeta}{\partial T}\frac{1}{2\zeta^2}\left(\frac{\alpha}{\sqrt{\alpha^2 - c^*_{\mathrm{M}^+}c^*_{\mathrm{a}^-}}} - 1\right) < 0. \qquad (19)$$

This temperature derivative always takes a negative value, since $\partial\zeta(T)/\partial T < 0$ and $\alpha > \sqrt{\alpha^2 - c^*_{\mathrm{M}+}c^*_{\mathrm{a}-}}$. Thus, the amount of ion pairs decrease and that of bare multivalent cations increases when temperature increases. This promotes the release of ion pairs as well as the adsorption of multivalent cations. Consequently, compaction is favored when temperature increases.

In this model, there is a finite discrepancy between the experimental results and the theoretical expectation. This discrepancy is not eliminated by adjusting parameters within a wide range. In fact, we can much better fit the theoretical lines in Fig. 2 with experimental data points. However, in this case, the temperature-dependence of the transition contradicts the experimental findings. This means that our model is not complete and needs some additional factors. For example, the binding free energy (which is a black box in this model) may depend on the salt concentration. In addition, the persistence length actually changes according to the salt concentration. In our experimental condition, in the presence of monovalent anions or divalent anions, this additional electrostatic persistence length would be much smaller than the intrinsic one, whereas, in the presence of trivalent anions, the elongation of the persistence length is not negligible according to the theories of Odijk (17) and Skolnick and Fixman (18),

$$l_{\mathrm{p}} = l_{\mathrm{p,o}} + l_{\mathrm{p,e}}, \qquad (20)$$

where l_{p} is the total persistence length, $l_{\mathrm{p,\,0}}$ is the intrinsic one, and $l_{\mathrm{p,e}} = (1 - \sum_{\mathrm{i}} z_{\mathrm{i}}\theta_{\mathrm{i}})^2/4\kappa^2 d^2$ is the additional electrostatic one. On the basis of the Flory formula, the additional free energy to the left-hand side in Eq. 17 is given as

$$\begin{aligned}\beta\Delta F_{\mathrm{ela,ele}} = {} & \frac{3}{2}\left(\tilde{\alpha}^2_{\mathrm{comp}} + \tilde{\alpha}^{-2}_{\mathrm{comp}}\right) - \frac{3}{2}\left(\tilde{\alpha}^2_{\mathrm{coil}} + \tilde{\alpha}^{-2}_{\mathrm{coil}}\right) \\ & -\frac{3}{2}(\alpha^2_{\mathrm{comp}} + \alpha^{-2}_{\mathrm{comp}}) + \frac{3}{2}(\alpha^2_{\mathrm{coil}} + \alpha^{-2}_{\mathrm{coil}}),\end{aligned} \qquad (21)$$

where $\tilde{\alpha}_{\mathrm{comp}} = l_{\mathrm{p,0}}/[N_{\mathrm{e}}^{1/2}2(l_{\mathrm{p,0}} + l_{\mathrm{p,e}})]$, $\tilde{\alpha}_{\mathrm{coil}} = 1$, $\alpha_{\mathrm{comp}} = l_{\mathrm{p,0}}/(N_0{}^{1/2}2l_{\mathrm{p,\,0}})$, and $\alpha_{\mathrm{coil}} = 1$ (The contour length is $L_{\mathrm{c}} = 2N_0 l_{\mathrm{p,0}} = 2N_{\mathrm{e}}(l_{\mathrm{p,0}} + l_{\mathrm{p,e}})$). The corrected phase boundary is shown as the dotted line in Fig. 3 *c*. As shown in the figure, the corrected phase boundary approaches slightly toward the experimental one. Furthermore, a cluster other than a simple pair may have a significant contribution. The estimation of ζ is another delicate problem. In the integrand of ζ, we adopt a considerably smaller value as the effective radius of small ions, than is usually expected. It is remarkable that the effective dielectric constant for a close separation of ions may be different from that at a macroscopic scale. In fact, when we effectively decrease the dielectric constant in the integrand of ζ by decreasing the maximum separation of the ion pair, a much larger radius of small ions gives almost the same results as in Figs. 2 and 4.

In plasma physics, it is well known that an ionic cluster such as a dipole plays a crucial role in the conductor-insulator transition (or Kosterlitz-Thouless transition) in two-dimensional plasma, where the ions are symmetric. The contribution of ion pairing for the transition in an asymmetric system is an open problem. In this study, from experimental and theoretical aspects, we extended theoretical and experimental studies in an asymmetric system.

In addition, it is well known that small anions such as adenosine triphosphate and adenosine diphosphate exist in the intracellular space. Adenosine triphosphate provides energy by hydrolysis, and changes its valency to adenosine diphosphate in a molecular motor. In previous studies on life science, however, there has been no clear hypothesis on how the change in cell size is associated with the change in the valencies of such small anions. Our present findings may promote development in this area.

CONCLUDING REMARKS

In this study, we examined the contribution of co-ions to DNA compaction in the presence of multivalent cations. Based on the experimental results regarding co-ion valency, DNA compaction induced by multivalent cations was shown to be impaired in the presence of higher-valence anions. This trend in the transition should be attributed to the formation of an ionic bound cluster (dipolelike) structure between multivalent cations and co-ions. In principle, the multivalent cation can be paired with co-ions in a cluster structure both in the bulk region and on the surface of unfolded DNA, from the point of view of the electroneutralization of DNA. Furthermore, the scenario of ion pairing is consistent with the experimental results regarding temperature-dependence, which suggests that compaction is associated with a gain in entropy and a loss in enthalpy. We have showed that, based on the model with ion pairing, the gain in entropy of small ions overcomes other entropic contributions.

We thank Professor D. Andelman at Tel Aviv University for a fruitful discussion.

This work was partly supported by Japan Society for the Promotion of Science under a Grant-in-Aid for Creative Scientific Research (project No. 18GS0421), and by the Ministry of Education, Culture, Sports, Science and Technology of Japan (grant No. 17076007). T.S. is supported by a Research Fellowship from Japan Society for the Promotion of Science for Young Scientists (grant No. 17-1618).

REFERENCES

1. Verwey, E. J. W., and J. T. G. Overbeek. 1948. Theory of the Stability of Lyophobic Colloids. Marcel Dekker, Elsevier, New York.
2. Israelachivili, J. 1991. Intermolecular and Surface Forces. Academic Press, London.
3. Wilson, R. W., and V. A. Bloomfield. 1979. Counterion-induced condensation of deoxyribonucleic acid. A light-scattering study. *Biochemistry.* 18:2192–2196.
4. Widom, J., and R. L. Baldwin. 1980. Cation-induced toroidal condensation of DNA studies with $Co^{3+}(NH_3)_6$. *J. Mol. Biol.* 144:431–453.
5. Yoshikawa, K., M. Takahashi, V. V. Vasilevskaya, and A. R. Khokhlov. 1996. Large discrete transition in a single DNA molecule appears continuous in the ensemble. *Phys. Rev. Lett.* 76:3029–3031.
6. Gosule, L. C., and J. A. Schellman. 1976. Compact form of DNA induced by spermidine. *Nature.* 259:333–335.
7. Yoshinaga, N., K. Yoshikawa, and S. Kidoaki. 2002. Multiscaling in a long semiflexible polymer chain in two dimensions. *J. Chem. Phys.* 116:9926–9929.
8. Murayama, H., and K. Yoshikawa. 1999. Thermodynamics of the collapsing phase transition in a single duplex DNA molecule. *J. Phys. Chem. B.* 103:10517–10523.
9. Matulis, D., I. Rouzina, and V. A. Bloomfield. 2000. Thermodynamics of DNA binding and condensation: isothermal titration calorimetry and electrostatic mechanism. *J. Mol. Biol.* 296:1053–1063.
10. Saito, T., T. Iwaki, and K. Yoshikawa. 2005. Why is the compact state of DNA preferred at higher temperature? Folding transition of a single DNA chain in the presence of a multivalent cation. *Europhys. Lett.* 71:304–310.
11. Debye, P. W., and E. Hückel. 1923. The theory of the electrolyte. *Phys. Z.* 24:185–206.
12. MacGillivray, A. D. 1972. Upper bounds on solutions of the Poisson-Boltzmann equation near the limit of infinite dilution. *J. Chem. Phys.* 56:80–83.
13. Oosawa, F. 1971. Polyelectrolytes. Marcel Dekker, New York.
14. Manning, G. S. 1978. The molecular theory of polyelectrolyte solutions with applications to the electrostatic properties of polynucleotides. *Q. Rev. Biophys.* 11:179–246.
15. Saito, T., T. Iwaki, and K. Yoshikawa. 2008. DNA compaction induced by neutral polymer is retarded more effectively by divalent anion than monovalent anion. *Chem. Phys. Lett.* 465:40–44.
16. Bjerrum, N. 1926. Analysis of ionic association. *Kgl. Dan. Vidensk. Selsk. Mat.-Fys. Medd.* 7:1–48.
17. Odijk, T. 1977. Polyelectrolytes near the rod limit. *J. Polym. Sci. Polym. Phys. Ed.* 15:477–483.
18. Skolnick, J., and M. Fixman. 1977. Electrostatic persistence length of a wormlike polyelectrolyte. *Macromolecules.* 10:944–948.
19. Burak, Y., G. Ariel, and D. Andelman. 2004. Competition between condensation of monovalent and multivalent ions in DNA aggregation. *Curr. Opin. Colloid Interface Sci.* 9:53–58.
20. Yamasaki, Y., Y. Teramoto, and K. Yoshikawa. 2001. Disappearance of the negative charge in giant DNA with a folding transition. *Biophys. J.* 80:2823–2832.
21. Levin, Y. 2002. Electrostatic correlations: from plasma to biology. *Rep. Prog. Phys.* 65:1577–1632.
22. Shklovskii, B. I. 1998. Wigner crystal model of counterion induced bundle formation of rodlike polyelectrolytes. *Phys. Rev. Lett.* 82:3268–3271.
23. Grönbech-Jensen, N., R. J. Mashl, R. F. Bruinsma, and W. M. Gelbart. 1997. Counterion-induced attraction between rigid polyelectrolytes. *Phys. Rev. Lett.* 78:2477–2480.
24. Rouzina, I., and V. A. Bloomfield. 1996. Macroion attraction due to electrostatic correlation between screening counterions. 1. Mobile surface-adsorbed ions and diffuse ion cloud. *J. Phys. Chem.* 100:9977–9989.
25. Stevens, M. J. 1996. Bundle binding in polyelectrolyte solutions. *Phys. Rev. Lett.* 82:101–104.
26. Ha, B. -Y., and A. J. Liu. 1997. Counterion-mediated attraction between two like-charged rods. *Phys. Rev. Lett.* 79:1289–1292.
27. Golestanian, R., M. Kardar, and T. B. Liverpool. 1999. Collapse of stiff polyelectrolytes due to counterion fluctuations. *Phys. Rev. Lett.* 82:4456–4459.
28. Kornyshev, A. A., D. J. Lee, S. Leikin, and A. Wynveen. 2007. Structure and interactions of biological helices. *Rev. Mod. Phys.* 79:943–996.
29. Yoshikawa, K., and Y. Matsuzawa. 1995. Discrete phase transition of giant DNA dynamics of globule formation from a single molecular chain. *Physica D.* 84:220–227.